Desalination and Water Treatment
www.deswater.com

doi:10.5004/dwt.2017.20208

72 (2017) 30–40
April

Kinetic and isothermal studies of manganese (VII) ions removal using Amberlite IRA-420 anion exchanger

M.S. Mohy Eldin[a,c,*], K.A. Alamry[b], M.A. Al-Malki[a]

[a]*Chemistry Department, Faculty of Science, University of Jeddah, Asfan P. O. Box 80203, Jeddah 21589, Saudi Arabia, Tel. 00966569006640, email: mmohyeldin@srtacity.sci.eg (M.S. Mohy Eldin), mohammed_almalki1992@hotmail.com (M.A. Al-Malki)*
[b]*Chemistry Department, Faculty of Science, King Abdul Aziz University, Jeddah 21589, Saudi Arabia, email: kaalamri@kau.edu.sa (K.A. Alamry)*
[c]*Polymer Materials Research Department, Advanced Technology and New Materials Research Institute, SRTAC, New Borg El-Arab City 21934, Alexandria, Egypt*

Received 11 May 2016; Accepted 28 August 2016

ABSTRACT

Anion exchanger (Amberlite IRA-420; AMB) has been used in the removal of permanganate ions from potassium permanganate contaminated water. Operational conditions such as permanganate concentration, adsorption time, adsorption temperature, adsorption pH, agitation speed, and finally adsorbent dosage have been investigated, and its impact on the removal process efficiency has been presented. Moreover, the kinetic and equilibrium results obtained for permanganate ions sorption with different initial concentrations onto AMB were analyzed. Kinetic modeling analysis with three different types of kinetic sorption models (pseudo-first-order, pseudo-second-order, and simple Elovich models) was applied to simulate the permanganate ions sorption data. The analysis of the kinetic data indicated that the sorption was a second-order process. An ion-exchange mechanism may have existed in the permanganate ions-sorption process with AMB. The permanganate ions uptake by AMB was quantitatively evaluated with equilibrium sorption isotherms. To describe the isotherms mathematically, the experimental data of the removal equilibrium were correlated with the Langmuir, Freundlich, Temkin, and Dubinin–Radushkevich (D–R) isotherm models, and the applicability of these isotherm equations to the sorption systems was compared by the correlation coefficients. The maximum sorption capacities, determined from the Langmuir isotherm was 20.54 mg/g at 25°C. Moreover, diffusion mechanism of permanganate ions was described by different adsorption diffusion models. The diffusion rate equations inside particulate of Dumwald–Wagner and intraparticle models were used to calculate the diffusion rate. The actual rate-controlling step involved in the permanganate ions sorption process was determined by further analysis of the sorption data applying the kinetic expression given by Boyd.

Keywords: Anion exchanger; Adsorption; Permanganate ions; Kinetics; Equilibrium; Diffusion; Removal

1. Introduction

Manganese is an essential trace nutrient in all known forms of life. Manganese poisoning, however, has been linked to impaired motor skills and cognitive disorders. Higher levels of exposure to manganese in water are associated with increased intellectual impairment and reduced intelligence quotients in school-age children [1] Heavy metal wastewater exists in various industries such as metal finishing, electroplating, plastics, pigments and mining, which threatens to the environment and human lives severely. Therefore it is urgent to remove toxic heavy metals from waste water. Several treatment methods have been suggested, developed

*Corresponding author.

and used to remove heavy metals from wastewater. These methods [2–7] include chemical precipitation, ion exchange, cementation, coagulation and flocculation and membrane processes. However, these techniques have been found to be very expensive. So, we need effective and inexpensive processes for removal of heavy metals.

Adsorption techniques are widely used to remove certain classes of pollutants from wastewater [8–9].

Potassium permanganate is commonly used in multidiscipline processes as a strong oxidizing agent for oxidative treatment of a significant number of organic and inorganic compounds in soil and water solutions [10–19].

Up to our knowledge, few publications addressed the removal of permanganate ions. Adsorption is considered to be a cheap and efficient method for the removal of Mn (VII) from wastewater using different adsorbents such as activated orange peels powder [20], activated carbon [21–22], *Prosopis cineraria* leaf powder [23], and Millet husk [24].

The aim of this work is to study the removal of Mn (VII) ions from permanganates ions solution using strong anion exchanger of amine quaternary cross-linked styrene/divinylbenzene copolymer. Different operation conditions such as permanganate concentration, adsorption time, adsorption temperature, adsorption pH, agitation speed, and finally adsorbent dosage have been investigated, and its impact on the removal process efficiency has been presented. Moreover, the kinetic and isothermal results obtained for permanganate ions sorption with different initial concentrations were analyzed.

2. Materials and methods

2.1. Materials

Amberlite (IRA 420); A commercial Amberlite IRA-420 ion exchange resin was supplied by Rohm and Hass. It is an amine quaternary cross-linked styrene/divinylbenzene copolymer. Table 1 shows a summary of the resin properties [25].

Potassium permanganate ($KMnO_4$), minimum assay 99%, was supplied by Sigma Aldrich, Germany.

Table 1
Properties of the resin Amberlite IRA-420

Producer	Rohm and Haas
Functionality	$-N^+-(CH_3)_3$
Matrix type	Polystyrene-DVB
Standard ionic form	Cl^-
Total exchange capacity(meq/g)	3.80
Bed Porosity	0.32
Wet resin density (g/cm^3)	1.15
Bed density (g/cm^3)	0.68
pH operating range	0–14
Maximum operating temperature	77°C
Mean wet nparticle radius(mm)	0.30–0.70

2.2. Preparation of basic permanganate solution

Potassium permanganate, the stock solution was prepared by dissolving 1 g in 1000 mL distilled water using magnetic stirrer. The permanganate concentrations in the supernatant and residual solutions were determined by measuring their absorbance using 1 cm light-path cell at Max wavelength 525 nm using UV- Visible spectrophotometer.

2.3. Standard curve of permanganate concentration

Varied Permanganate solution concentrations from 1 ppm to 100 ppm were prepared. The absorbance (A_{abs}) of the samples was measured using a UV-Visible spectrophotometer and plotted against their concentrations. From the slope, we can derive the following relation between absorbance and concentration;

$$\text{Concentration}(\text{ppm}) = A_{abs} X \text{ Constant}\left(\frac{1}{\text{Slope}}\right) \quad (1)$$

2.4. Adsorption experiment

The adsorption experiments were carried out in a batch process by using permanganate aqueous solution. The variable parameters namely; the initial permanganate concentration, the adsorbent amount, the contact time, and the adsorption temperature have been studied. The permanganate adsorption studies have been performed by mixing 0.1 g of wet Amberlite IRA 420 with 10 mL of 100 ppm permanganate. The mixture was agitated at R·T using magnetic stirrer for 30 min then left to settle for 1 min to separate the adsorbent out of the liquid phase. The permanganate concentration at ppm, before and after the adsorption, for each solution, was determined by measuring the absorbance at the maximum wavelength (λ_{max} = 525 nm) using UV-VIS spectrophotometer and multiply by 66.67 constant extracted from the slope of the standard curve. The permanganate removal percentage was calculated according to the following formula:

$$\text{Permanganate removal}(\%) = \left[\frac{(C_0 - C_t)}{C_0}\right] \times 100 \quad (2)$$

where C_0 and C_t (mg L^{-1}), are the initial at zero time and the final concentration of permanganate at a specific time, respectively.

2.5. Sorption kinetic models

Three frequently used kinetics models namely; the pseudo-first-order, the pseudo-second-order, and finally the Elovich have been used to follow up the kinetics of the adsorption process.

2.5.1. Pseudo-first-order model

Langergren and Svenska [26] correlated the adsorption rate to the adsorption capacity to follow up the kinetic of the adsorption process from solution onto solid surface using the following linear equation:

$$\ln\left(q_e - q_t\right) = \ln q_e - k_1 t \tag{3}$$

The first order reaction rate constant k_1 (min^{-1}) obtained from the slope of the linear line resulted from plotting $\ln(q_e - q_t)$ versus time. The adsorbed amounts (mg/g) at time t (min) defined as q_t and as q_e at equilibrium.

2.5.2. Pseudo-second-order model

The pseudo-second-order model describes the kinetic of the chemisorption process using the following linear form equation [27]:

$$\frac{t}{q_t} = \frac{1}{\left(1 + k_2 q_e^{\,2}\right)} + \frac{t}{q_e} \tag{4}$$

The second-order reaction rate equilibrium constant k_2 (g/mg min) and q_e values can be determined from the slope and intercept of the plot of t/q_t against time (min).

2.5.3. Elovich model

Despite the routine use of the simple Elovich model in describing the kinetics of chemisorption of gas onto solid systems, it has been also utilized in the recent times to monitor the pollutants adsorption from aqueous solutions. The simple form equation of the Elovich model is [28]:

$$q_t = \alpha + \beta \ln t \tag{5}$$

Linear relationship normally obtained by plotting q_t versus ln t where the slope and the intercept of the obtained line expressed the initial sorption rate (α; mg/g min), and the extent of surface coverage and activation energy for chemisorption (β; g/mg).

2.6. Sorption mechanisms

2.6.1. Dumwald–Wagner model

The Dumwald–Wagner model describes the diffusion of adsorbate inside particulate by the following equation [29]:

$$\log\left(1 - F^2\right) = -\left(\frac{K}{2.303}\right) * t \tag{6}$$

Plotting of log ($1–F^2$) versus t resulted in a straight line. The diffusion rate constant is K, and the adsorption percent is F which calculated by (q_t/q_e).

2.6.2. Intraparticle model

The identification of the adsorption mechanism usually needs to use the intraparticle model [30].

$$q_t = k_a t^{1/2} + C \tag{7}$$

Plotting the adsorption capacity q_t against $t^{1/2}$ normally gives dependences with two linear segments. The intraparticle diffusion rate (k_d) and the thickness of the boundary layer (C) were calculated from the slope and the intercept of the second linear part, respectively.

2.6.3. Boyd model

Boyd et al. identify the rate-controlling step involved in the adsorption step using the following equations [31].

$$F = 1 - \left(\frac{6}{\pi^2}\right)\exp\left(-B_t\right) \tag{8}$$

The percentage of solute adsorbed at time t (F) given by the following equation:

$$F = \frac{q_t}{q_a} \tag{9}$$

The amount of adsorbed solute (mg/g) at any time t and at an infinite time are defined as (q_t) and (q_α).

B_t is a mathematical function of F and can be calculated for each value of F using Eq. (10) obtaining from substituting Eq. (8) into Eq. (9). Plotting B_t values versus time will provide useful information to distinguish between external transport- and intraparticle-transport controlled rates of sorption based on the linearity of this plot.

$$B_t = -0.4978 - Ln\left(1 - \frac{q}{q_a}\right) \tag{10}$$

2.7. Sorption isotherm models

The sorption isotherm models deal with the main factors affecting the interaction between the adsorbent surface and the adsorbate. These factors could be mentioned as:

- The homogeneity of the adsorption sites distribution,
- The limitation of adsorption levels (layers), and
- The indirect adsorbent/adsorbate interactions.

2.7.1. Freundlich isotherm

The Freundlich isotherm model, the oldest one, assumed the heterogeneity of the adsorbent surface and the formation of multilayer adsorbate [32]. The linear mathematical form of the model is expressed as:

$$\ln q_e = \ln K_F + \frac{1}{n_f} Ln C_e \tag{11}$$

Plotting ln q_e versus ln C_e a straight line with slope $1/n_f$ and intercept ln K_F is obtained. The q_e is defined as the amount of ions sorbed at equilibrium (mg/g). The adsorbate concentration at equilibrium is C_e (mg/L). The K_F is an indicator of the adsorption capacity and n_f is an indicator of the adsorption effectiveness.

2.7.2. Langmuir isotherm

The Langmuir isotherm model postulated the formation of monolayer adsorbate onto an entirely homogeneous distribution of adsorption sites onto the adsorbent

surface neglecting the interaction between the adsorbate molecules [33].

$$\frac{C_e}{q_e} = \frac{1}{q_m}K + \frac{C_e}{q_m} \tag{12}$$

Plotting of C_e/q_e against C_e presenting a straight line of slope $1/q_m$ and intercept $1/q_mK$. The Langmuir constants; the maximum adsorption capacity q_m (monolayer capacity; mg/g) and the energy of adsorption K (L/mg) can be calculated from the slope and the intercept, respectively.

To predict the favorableness of the adsorption system, a dimensionless separation factor (R_L) was calculated (Eq. (13)) to identify the isotherm shape [34].

$$R_L = \frac{1}{(1+KC_0)} \tag{13}$$

C_0 is defined as the permanganate ions initial concentration (mg/L).

2.7.3. D–R isotherm

For describing the adsorption of single solute systems, the D–R isotherm is usually used. The D–R isotherm in one hand considering the formation of monolayer adsorbate, as the Langmuir isotherm, but on the other hand, considering the heterogeneity of the adsorbent surface and unequal adsorption potential as the Freundlich isotherm model [35]. The D–R isotherm model linear expression is:

$$\ln q_e = \ln V_m' - K'\varepsilon^2 \tag{14}$$

The adsorption capacity at equilibrium is q_e (mg/g), the D–R maximum sorption capacity is V_m' (mg/g), the adsorption energy constant is K' (mol²/kJ²), and the Polanyi potential is ε.

$$\varepsilon = RT\ln\left(1+\frac{1}{C_e}\right) \tag{15}$$

The R is defined as the gas constant (8.314×10^{-3} kJ/mol K), and T is the temperature (K). The K' is the energy required to transfer of adsorbate molecules from the solution phase to the surface of the solid phase. The nature of the adsorption process, physical or chemical features, extracted from the energy value [36] which calculated according to the following equation [37].

$$E = \left(2K'\right)^{-0.5} \tag{16}$$

2.7.4. Temkin isotherm

The Temkin isotherm considers the effect of the indirect interactions between the adsorbent and adsorbate, on the adsorption process. That indirect interaction leads to decreases linearly the adsorption's heat of all molecules in a layer with coverage [38]. The linear mathematical form of the model considered as follows [39]:

$$q_e = BLnK_T + BLnC_e \tag{17}$$

Plotting q_e against ln C_e a straight line, indicating the value of B constant from its slope and the value of K_T constant from its intercept, is obtained.The Temkin constant (K_T) is defined as the maximum binding energy equilibrium binding constant and (B) is the heat of sorption related constant.

3. Results and discussion

3.1. Adsorption process

A standard curve of permanganate concentration is presented in Fig. 1. From the curve's slope, the constant has been calculated and was fond equal to 66.67.

Factors affecting the permanganate ions removal process using Amberlite have been investigated. The factors considered are the permanganate ions concentration, the adsorption's time, the adsorption's temperature, the adsorption's pH, the agitation speed, and the adsorbent dosage. The impact of those factors on the removal process efficiency has been presented.

3.1.1. Effect of the permanganate concentration

The effect of variation the permanganate concentration on its removal percentage and the capacity of adsorbent have been presented in Fig. 2. From the illustrated results, it is clear that the removal percentage has not been affected significantly by variation of the permanganate concentration. The removal percentages ranged between 86% and 93%.

On the other hand, a clear increase of the adsorbent capacity has been observed. That increment could be explained by increase the concentration gradient between the permanganate solution phase and the adsorbent solid phase. That gradient acting as the driving force of the permanganate molecules towards the Amberlite surface and the interior in addition to the hydrophobic and the ions exchange interactions. The individual or the synergetic effect of all the three factors leads finally to the obtained results.

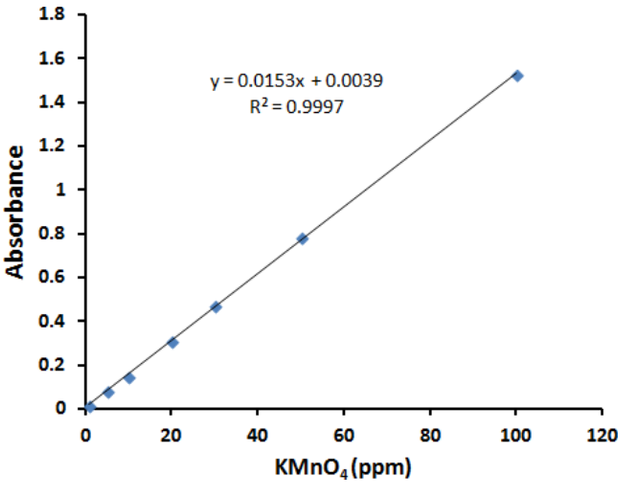

Fig. 1. Standard curve for Permanganate concentration.

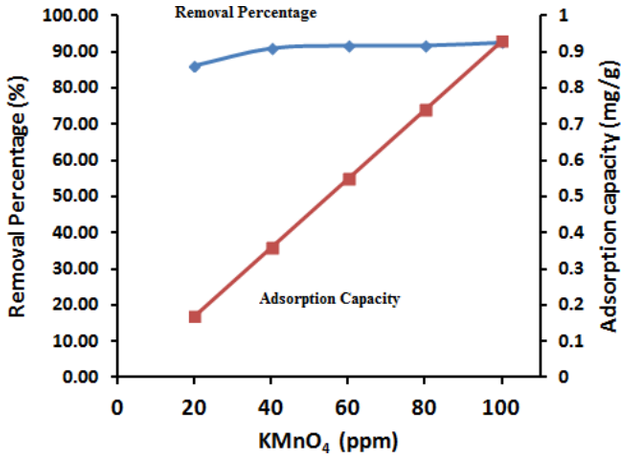

Fig. 2. Effect of Permanganate concentration on the removal percentage and adsorbent capacity.

3.1.2. Effect of the adsorption time

Fast adsorption is one of the key features of the efficient adsorbent. Accordingly, the effect of variation the adsorption time on the removal percentage and the capacity of adsorbent has been presented in Fig. 3.

From the illustrated data in Fig. 3, it is clear that fast adsorption process has been recognized through the removal of 92% of the permanganate ions within 15 min where its concentration sharply dropped to 8 ppm. The rate of the adsorption process starts to lower after. That behavior expected since the remaining permanganate ions in the solution phase became very low and so the ions exchange site over the amberlite beads (solid phase) which represent the driving forces of the adsorption process. On the other hand, adsorbent capacity shows a similar behavior to the permanganate removal (%) where the capacity has been increased rapidly in the early time of the adsorption process then started to level off. The reasons have been mentioned above.

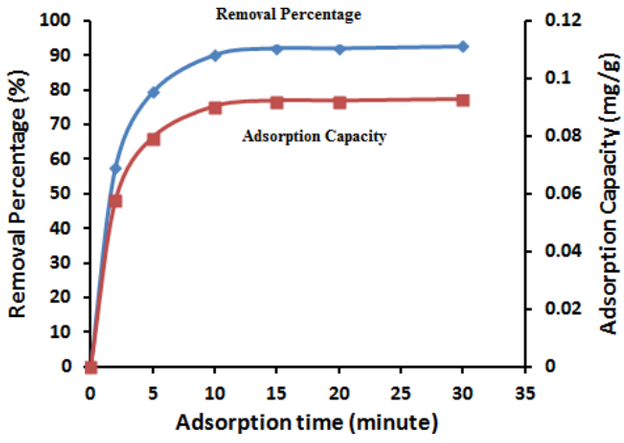

Fig. 3. Effect of adsorption time on the removal percentage and adsorbent capacity.

3.1.3. Effect of the adsorption temperature

Energy consumption is one of the main concerns while performing any adsorption process from the efficiency and the practical points of view. The effect of variation the adsorption's temperature within 5 min adsorption time on the removal percentage and the capacity of adsorbent from 100 ppm permanganate ions solution have been presented in Table 2.

From the tabulated results, it is clear that the adsorption's temperature has no significant effect on the adsorption process which reflects its slightly endothermic nature. Both of the removal percentage and the adsorbent capacity have been increased very slightly with increasing the adsorption's temperature. That slight increment could be explained by the high affinity between the permanganate liquid phase and the Amberlite solid phase. That affinity consequently reduces the main effect of the adsorption temperature in facilitating the diffusion of the adsorbed permanganate ions from the liquid phase to the beads solid phase. Such behavior has been considered as an advantage for the adsorption process from the cost point of view.

3.1.4. Effect of the adsorption pH

Aqueous solution pH is a critical parameter as it strongly affects the metal sorption, the surface charge of the adsorbent, the degree of ionization and the speciation of the adsorbate species [20]. The permanganate ions adsorption was carried out to optimize the pH for maximum removal efficiency. The pH of the solution varied from 2–7, at constant initial concentration, contact time, and temperature. No significant effect on the removal percentage and the adsorption capacity was observed upon variation of the permanganate ions solution pH. The removal percentages ranged between 92% and 94% within 30 min adsorption time at R·T (Table 3).

Table 2
Effect of adsorption temperature on the removal percentage and adsorption capacity

Temperature (C°)	Removal percentage (%)	Adsorption capacity (mg/g)
25	79.65	7.965
40	81.46	8.146
50	82.13	8.213
60	83.00	8.300

Table 3
Effect of adsorption pH on the removal percentage and adsorption capacity

pH	Removal percentage (%)	Adsorption capacity (mg/g)
2.0	91.55	9.16
4.0	92.30	9.23
5.0	93.10	9.31
7.0	94.00	9.4

The obtained results are agreed with the published results by Mahmoud et al. [22]. Unlike the ammonium ion (NH_4^+) and the primary, secondary, or tertiary ammonium cations, the quaternary ammonium cations are permanently charged, independent of the pH of their solution [40]. On the other hand, $KMnO_4$ undergoes in acidic–neutral pH conditions to produce Mn^{+2} and manganese dioxide as illustrated by Eqs. (18)–(19) [11].

In strong acidic condition:

$$MnO_4^- + 8H^+ + 5e^- \rightarrow Mn^{2+} + 4H_2O \quad (18)$$

In acidic-neutral condition:

$$MnO_4^- + 4H^+ + 3e^- \rightarrow MnO_2(s) + 2H_2O \quad (19)$$

According to Mahmoud et al. [22], in pH 1.0 solution, removal of $KMnO_4$ was found to proceed via anion exchange mechanism. At a pH 7.0, the $KMnO_4$ reduction product as Mn (II) was removed due to the possibility of complex formation. The same finding was earlier stated by Zhang et al. [21]. They found that permanganate was not adsorbed but reduced by activated carbon particles. The percent of reduction of permanganate was strongly pH-dependent. The reducing product of permanganate was mainly Mn^{2+}, which was adsorbed onto the activated carbon particles by surface complexation.

3.1.5. Effect of the agitation speed

The effect of variation the agitation speed from 100 to 300 rpm on the removal percentage and adsorption capacity of permanganate ions was studied. It was found that the removal percentage ranged from 78.6% to 79.86% while the adsorption capacity of the resin was found equal to 7.986 (mg/g) after 5 min contact time at 300 rpm compared with 7.86 (mg/g) at 100 rpm, respectively. The high affinity for the ion exchange site on the ion exchanger beads and the Mn (VII) ions in the solution eliminates the effect of the agitation speed to a great extent. That is considered as an advantage from the economic point of view based on saving energy.

3.1.6. Effect of the adsorbent dose

The effect of variation the adsorbent dose on the removal percentage and the capacity of the adsorbent have been studied and presented in Fig. 4. The illustrated results in Fig. 4. reveal that the permanganate ions removal (%) increases with increase the adsorbent dose. Within studied adsorption's time, 0.02 g of adsorbent has removed 78.5% of permanganate ions while 0.1 g has removed about 92% of permanganate ions. On the other hand, it is clear that the adsorbent's capacity decreases with increase the adsorbent's dose. It is logic enough since increase the adsorbent's dose increase the available active site for adsorption the permanganate ions. The rate of capacity decrease tends to level off due to the limitation of the available permanganate ions.

3.2. Sorption kinetic models

The kinetic study is important for an adsorption process because it depicts the uptake rate of the adsorbate and

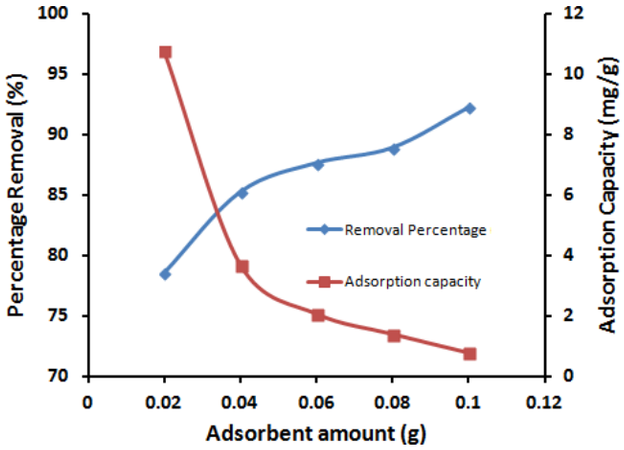

Fig. 4. Effect of adsorbent dose on the removal percentage and adsorbent capacity.

controls the remaining time of the whole adsorption process. So, three different kinetic models, pseudo-first-order, pseudo-second-order and Elovich, were selected in this study for describing the permanganate ions sorption process using AMB.

3.2.1. Pseudo-first-order model

The pseudo-first-order kinetic model was the earliest model about the adsorption rate based on the adsorption capacity. The first order reaction rate constant k_1 (min^{-1}) was obtained from the slope of the linear plot resulting from plotting ln ($q_e - q_t$) vs. time; Fig. 5. The values of the first-order rate constant k_1 and correlation coefficient, R^2 are tabulated in Table 4. From the table, it indicated that the correlation coefficients are good enough. However, the estimated values of q_e calculated from the equation differed from the experimental values (Table 4).

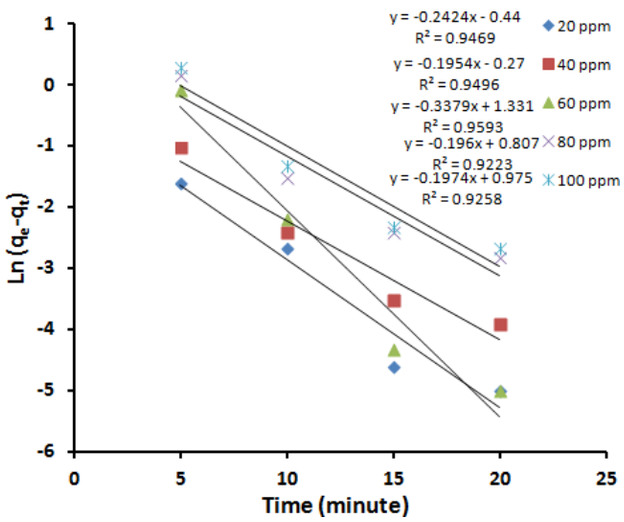

Fig. 5. First order plot for Permanganate ions removal using AMB.

Table 4
The values of the first-order-rate constants

C_0	K_1	$q_{cal.}$	$q_{exp.}$	R^2
20	–0.2468	0.644	1.807	0.9469
40	–0.195	0.76	3.650	0.9496
60	–0.342	3.78	5.513	0.9593
80	–0.196	2.24	7.360	0.9223
100	–0.197	2.65	9.300	0.9258

3.2.2. Pseudo-second-order model

The chemisorption kinetics can also be given by the pseudo-second-order rate. The pseudo-second-order kinetics applies to the experimental data. The plot of t/q_t versus t gave a linear relationship as illustrated in Fig. 6. From the figure the values of q_e calculated and k_2 can be determined from the slope and intercept of the plot respectively (Table 5). Also, the value of the correlation coefficients, R^2 was extracted. Based on linear regression ($R^2 \approx 1$) values, the kinetics of permanganate ions sorption on to AMB can be described well by the second-order equation; this suggests that the rate-limiting step in these sorption processes may be chemisorptions involving valent forces through the sharing or exchanging of electrons between sorbent and sorbate [31]. Additionally, comparing the values of q_e calculated resulted from the intersection point of the second-degree reaction kinetic curve with that obtained from the experimental data indicated that the second order rate expression fits the data most satisfactorily.

3.2.3. Elovich model

The simple Elovich model is one of the most useful models for describing the kinetics of chemisorption of gas onto solid systems. However recently it has also been applied to describe the adsorption process of pollutants from aqueous solutions. Fig. 7. illustrates the plot of q_t against ln t for the sorption of permanganate ions onto AMB. From the slope and intercept of the linearization of the simple Elovich equation, the estimated Elovich equation parameters were obtained (Table 6). The values of β are indicative of the number of sites available for adsorption while α values are the adsorption quantity when ln t is equal to zero; i.e., the adsorption quantity when t is 1 h. This value is helpful in understanding the adsorption behavior of the first step [32]. Also, from the figure, it was declared that the Elovich equation does not fit well with the experimental data since the correlation coefficients are very low.

3.3. Sorption mechanisms

Since the determination of adsorption mechanism is required for design purposes and the previously mentioned models could not identify a diffusion mechanism, so we are going to discuss different adsorption diffusion models in the

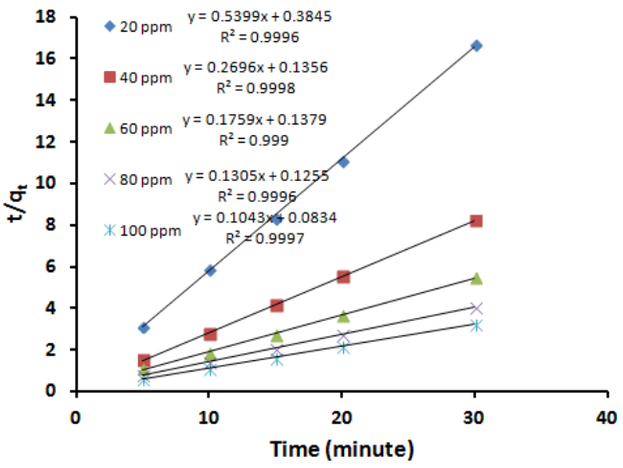

Fig. 6. Second order plot for Permanganate ions removal using AMB.

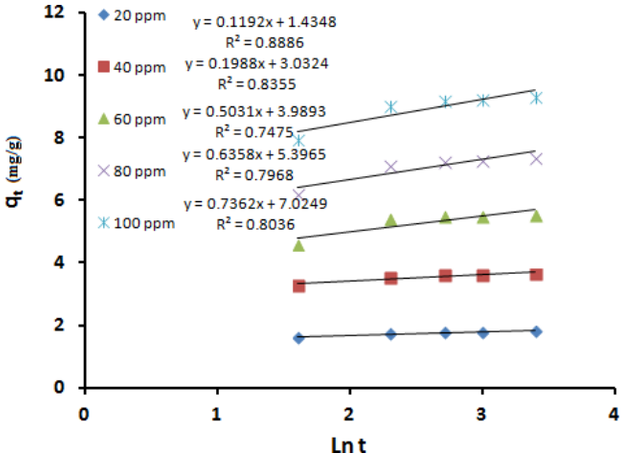

Fig. 7. Simple Elovich plot for Permanganate ions removal using AMB.

Table 5
The values of the second-order-rate constants

C_0	K_2	q_{cal}	$q_{exp.}$	R^2
20	0.38454	1.85	1.807	0.999
40	0.13565	3.71	3.650	0.999
60	0.13792	5.69	5.513	0.999
80	0.12554	7.7	7.360	0.999
100	0.08335	9.6	9.300	0.999

Table 6
Simple Elovich model constants

α (mg/g min)	β (g/mg)
1.441	0.119
3.032	0.199
4.004	0.503
5.397	0.636
7.025	0.736

following. It is known that a typical liquid/solid adsorption involves film diffusion, intraparticle diffusion, and mass action. For physical adsorption, mass action is a very rapid process and can be negligible for kinetic study. Thus, the kinetic process of adsorption is always controlled by liquid film diffusion or intraparticle diffusion, i.e., one of the processes should be the rate limiting step [33]. Therefore, adsorption diffusion models are mainly constructed to describe the process of film diffusion and intraparticle diffusion. To illuminate the diffusion of permanganate ions through AMB, the diffusion rate equation inside particulate of Dumwald–Wagner and intra-particle models were used to calculate the diffusion rate. On the other hand concerning the external mass transfer, Boyd model was examined to determine the actual rate-controlling step for the permanganate ions adsorption.

The linear plot of log $(1 - F^2)$ versus t indicates the applicability of Dumwald–Wagner kinetic model (Fig. 8). The diffusion rate constants for permanganate ions diffusion inside AMB were tabulated in Table 7.

The intraparticle diffusion plot for permanganate ions adsorption onto AMB was given in Fig. 9. Two separated linear portions that represent each line could be observed from the figure. These two linear portions in the intraparticle model suggest that the adsorption process consists of both surface adsorption and intraparticle diffusion. While the initial linear portion of the plot is the indicator of boundary layer effect, the second linear portion is due to intraparticle diffusion [34]. The intraparticle diffusion rate (k_d) was calculated from the slope of the second linear portion

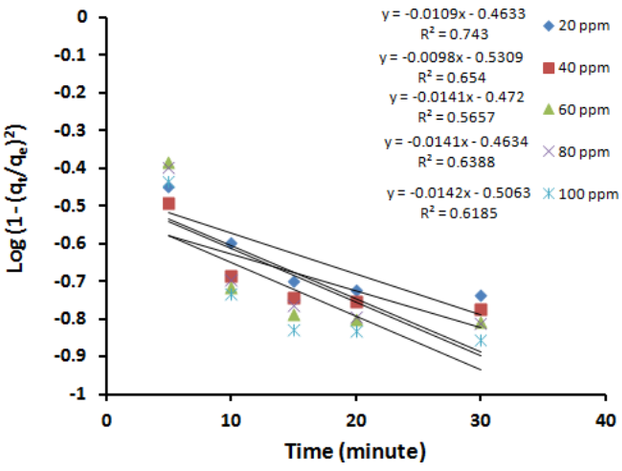

Fig. 8. Dumwald–Wagner plot for Permanganate ions removal using AMB.

Table 7
Dumwald–Wagner diffusion rate constants

C_o	K	R^2
20	0.025	0.743
40	0.0226	0.654
60	0.0325	0.5657
80	0.0325	0.6388
100	0.0327	0.685

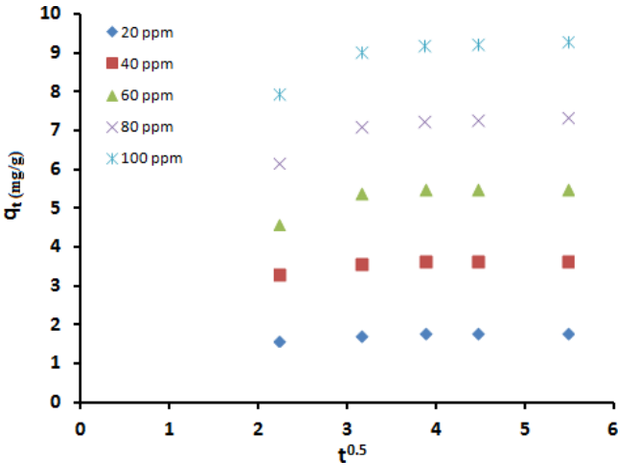

Fig. 9. Intraparticle diffusion plot for Permanganate ions removal using AMB.

(Table 8). The values of C give an idea about the thickness of the boundary layer. The larger the intercept, the greater is the boundary layer effect [35].

To characterize what the actual rate-controlling step involved in the permanganate sorption process, the sorption data were further analyzed by the kinetic expression given by Boyd et al. [36]. The value of B_t can be calculated for each value of F using Eq. (10). The calculated B_t values were plotted against time as shown in Fig. 10. The linearity

Table 8
The intraparticle diffusion constants

C_o	K_d	C	R^2
20	0.028	1.663	0.6456
40	0.036	3.462	0.837
60	0.037	5.316	0.5424
80	0.089	6.888	0.8956
100	0.109	8.728	0.8686

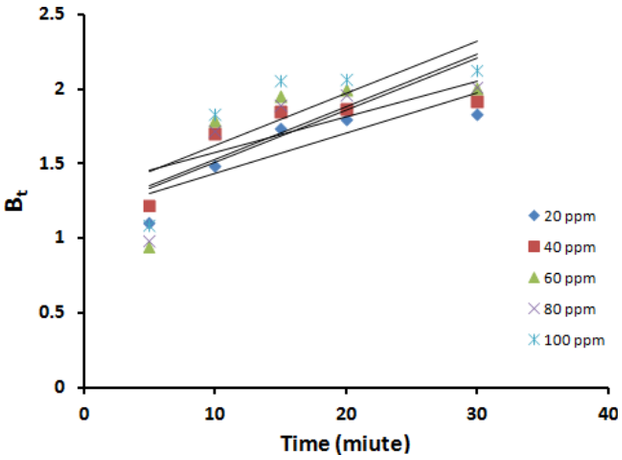

Fig. 10. Boyd expression of the sorption of Permanganate ions using AMB.

of this plot will provide useful information to distinguish between external transport- and intraparticle-transport controlled rates of sorption. Fig. 10 demonstrates the plot of B_t versus t, which was a straight line that does not pass through the origin, indicating that film diffusion governs the rate limiting process [37].

3.4. Sorption isotherm models

Sorption isotherms are mathematical models that describe the distribution of adsorbate species among solid and liquid phases, and they are thus important for chemical design. The results obtained for the sorption of permanganate ions onto AMB were analyzed with the well-known Freundlich, Langmuir, Temkin, and Dubinin–Radushkevich (D–R) models. The sorption data obtained for equilibrium conditions were analyzed with the linear forms of these isotherms.

3.4.1. The Freundlich isotherm

The Freundlich isotherm is a widely used equilibrium isotherm model but provides no information on the monolayer sorption capacity, in contrast to the Langmuir model [38,39]. The Freundlich isotherm model assumes neither homogeneous site energies nor limited levels of sorption. The Freundlich model is the earliest known empirical equation and has been shown to be consistent with the exponential distribution of active centers, which is characteristic of heterogeneous surfaces [40]. The values of Freundlich constants n_f and K_F, estimated from the slope and intercept of the linear plot (Fig. 11.) were 0.83 and 0.8023, respectively. From the estimated values of n_f, it was found that $n_f < 1$ dictated less favorable sorption for permanganate ions with the AMB beads [41].

3.4.2. The Langmuir model

The Langmuir model is valid for monolayer sorption onto entirely homogeneous surface with a finite number of identical sites and with a negligible interaction between adsorbed molecules. According to the R^2 value, which is regarded as a measure of the experimental data fitting for the isotherm model applying, the Langmuir equation for the sorption process of permanganate ions, the R^2 value obtained is 0.9327 (Fig. 12). That indicates a good mathematical fit. The Langmuir parameters for permanganate ions removal, q_m, and K were calculated from the slope and intercept of Fig. 12. The calculated values are 20.54 (mg/g) and 23.64 (L/mg), respectively. This indicates that the AMB was highly efficient for permanganate ions removal and had a moderately high energy of sorption (23.64 L/mg).

On the other hand, the essential characteristics of the Langmuir isotherm are defined by a dimensionless separation factor (R_L) that is indicative of the isotherm shape, which predicts whether an adsorption system is favorable or unfavorable. The calculated values of R_L for permanganate ions removal (Table 9) show favorable adsorption because the R_L values fall between 0 and 1 [42]. That again confirms that the Langmuir isotherm was favorable for the sorption of permanganate ions onto AMB under the conditions used in this study.

Langmuir and Freundlich isotherms are insufficient to explain the physical and chemical characteristics of adsorption.

3.4.3. The D–R isotherm

The D–R isotherm is commonly used to describe the sorption isotherms of single solute systems. The D–R isotherm, apart from being an analog of the Langmuir iso-

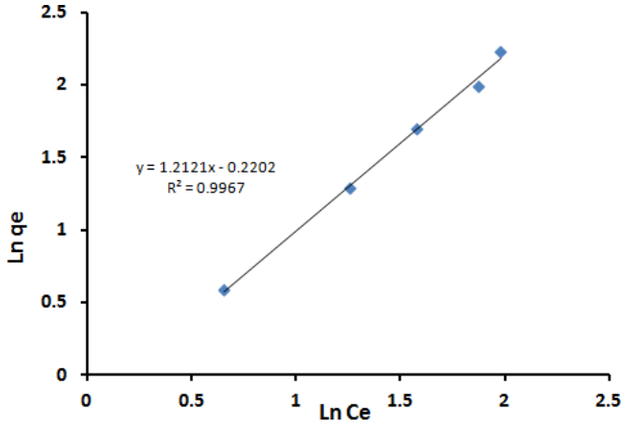

Fig. 11. Freundlich isotherm for the sorption of Permanganate ions using AMB.

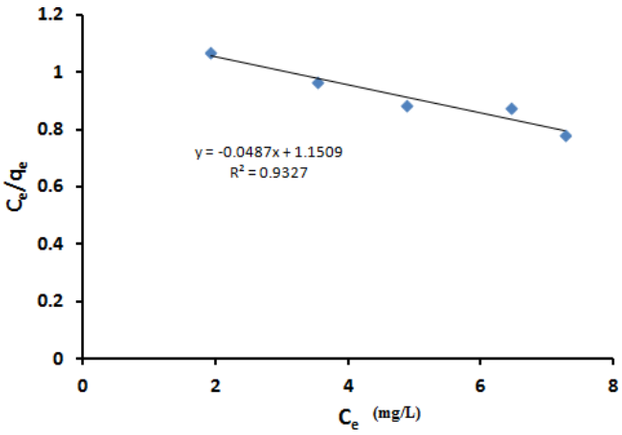

Fig. 12. Langmuir isotherm for the sorption of Permanganate ions using AMB.

Table 9
R_L values for different permanganate ions adsorption using AMB

C_0	R_L
20	0.00211
40	0.00106
60	0.0007
80	0.00053
100	0.00042

therm, is more general than the Langmuir isotherm because it rejects the homogeneous surface or constant adsorption potential. The D–R isotherm model was applied to the equilibrium data obtained from the empirical studies for permanganate ions removal with AMB to determine the nature of the sorption processes (physical or chemical). A plot of ln q_e against ε^2 is given in Fig. 13. The D–R plot yields a straight line with the R^2 values equal to 0.9024, and this indicates that the D–R model is less fits the experimental data in comparison with the Freundlich and the Langmuir isotherm models. According to the plotted D–R isotherm, the model parameters V_m', K', and E are equal to 8.47 mg/g, 1.53 mol^2/kJ^2, and 0.57 kJ/mol, respectively. The calculated adsorption energy (E < 8 kJ/mol) indicates that the permanganate ions sorption processes could be considered physisorption in nature [43]. Therefore, it is possible that physical means such as electrostatic forces played a significant role as sorption mechanisms for the sorption of permanganate ions in this work.

3.4.4. The Temkin isotherm

The Temkin isotherm considers the effects of indirect adsorbent/adsorbatee interactions on the adsorption process. The heat of adsorption of all molecules in a layer decreases linearly with coverage because of adsorbent/adsorbatee interactions. According to Fig. 14, the calculated value of K_T is 0.6464 L/g, and this represents the equilibrium binding constant corresponding to the maximum binding energy; however, constant B, which is 5.345 J/mol, is related to the heat of sorption.

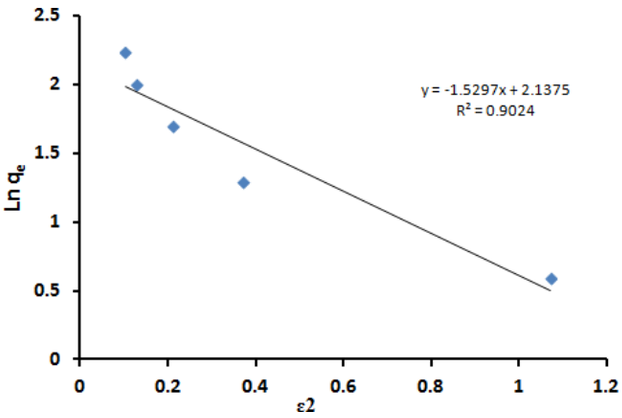

Fig. 13. D–R isotherm for the sorption of Permanganate ions using AMB.

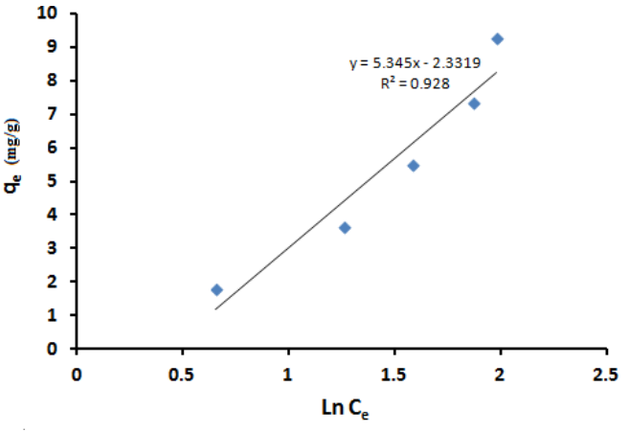

Fig. 14. Temkin isotherm for the sorption of Permanganate ions using AMB.

Table 10
R^2 Values for Permanganate removal with the different studied equilibrium isotherms

Isotherm model	R^2
Freundlich	0.9967
Langmuir	0.9327
D–R	0.9024
Temkin	0.9280

Finally, all the R^2 values obtained from the four equilibrium isotherm models applied to permanganate ions sorption on AMB are summarized in Table 10. The Freundlich model yielded the highest R^2 value (0.9967), and this showed that permanganate ions sorption on the AMB was best described by this model which assumes neither homogeneous site energies nor limited levels of sorption.

4. Conclusion

Successful adsorption of permanganate ions from aqueous solution has been achieved using Amberlite IRA-420 anion exchanger (AMB). Variation of the permanganate ions and the adsorbent dosage was found effective and determined in controlling the both the removal percentage and the adsorption capacity. Variation of the agitation speed and the adsorption temperature and pH were found not significant. These findings are very profitable from the economical point of view. The bench-scale studies carried out for permanganate ions removal with AMB showed a moderate sorption capacity (20.54 mg/g) at 25°C according to the Langmuir isotherm. Among the four adsorption isotherms tested, The Freundlich model yielded the highest R^2 value (0.9967), and this showed that permanganate ions sorption on the AMB was best described by this model which assumes neither homogeneous site energies nor limited levels of sorption.

The kinetics of the permanganate ions sorption rate was best explained by the pseudo-second-order kinetic equation. The kinetic model confirmed that the ion-exchange mechanism played a significant role in all the studied permanganate ions sorption systems.

Moreover, diffusion mechanism of permanganate ions was described by different adsorption diffusion models. The diffusion rate equations inside particulate of Dumwald–Wagner and intraparticle models were used to calculate the diffusion rate. E are less than 8 kJ/mol, so the sorption process has a physical nature. To determine what was the actual rate-controlling step involved in the permanganate ions sorption process, the sorption data was further analyzed by the kinetic expression given by Boyd. The obtained results indicate that the film diffusion is the rate-limiting process.

References

[1] World Health Organization (WHO), Guidelines for Drinking – Water Quality, 3rd ed., Recommendations, Geneva, 2004, 1,334.
[2] T. Robinson, B. Chandran, P. Nigam, Removal of dyes from a synthetic textile dye effluent by biosorption on apple pomace and wheat straw, Water Res., 36 (2002) 2824–2830.
[3] K.C. Sekhar, N.S. Chery, C.T. Kamala, J.V. Rao, V. Balaram, Y. Anjaneyuly, Risk assessment and pathway study of arsenic in industrially contaminated sites of Hyderabad: A case study, Environ. Int., 29 (2003) 601–611.
[4] T.A. Kurnivan, G.Y. Chan, W.H. Lo, S. Babels, Comparisons of low-cost adsorbents for treating wastewaters laden with heavy metals, Sci. Total Environ.; 2006.
[5] V.M. Luna-Pabello, T. Pandiyan, A.E. Dominguez, Kinetic model for wastewater treatment: spectroscopic determination of pollutants, Res. J. Chem. Environ., 10 (2006) 67–79.
[6] M. Uysal, A. Irfan, Removal of Cr (VI) from industrial wastewaters by adsorption, J. Hazard. Mater., B-134 (2007) 149–156.
[7] A. Bhatnagar, A.K. Minocha, Conventional and non-conventional adsorbents for removal of pollutants from water-A review, Indian J. Chem. Tech., 13 (2006) 203–217.
[8] E. Demirbas, Heavy metal adsorption onto agro-based waste materials: a review, J. Hazard. Mater., 157 (2008) 220–229.
[9] M.d. Ahmaruzzaman, Adsorption of phenolic compounds on low-cost adsorbents: A review, Adv. Colloid Interf. Sci., 143 (2008) 48–67.
[10] R.H. Waldemer, P.G. Tratnyek, Kinetics of contaminant degradation by permanganate, Environ. Sci. Technol., 40 (2006) 1055–1061.
[11] R. Liu, H. Liu, X. Zhao, J. Qu, R. Zhang, Treatment of dye wastewater with permanganate oxidation and in situ formed manganese dioxides adsorption: Cation blue as model pollutant, J. Hazard. Mater., 176 (2010) 926–931.
[12] K.C. Huang, G.E. Hoag, P. Chheda, B.A. Woody, G.M. Dobbs, Kinetics and mechanism of oxidation of tetrachloroethylene with permanganate, Chemosphere, 46 (2002) 815–825.
[13] E. Rodríguez, G.D. Onstad, T.P.J. Kull, J.S. Metcalf, J.L. Acero, U.V. Gunten, Oxidative elimination of cyanotoxins: Comparison of ozone, chlorine, chlorine dioxide and permanganate, Water Res., 41 (2007) 3381–3393.
[14] D. He, X. Guan, J. Ma, X. Yang, C. Cui, Influence of humic acids of different origins on oxidation of phenol and chlorophenols by permanganate, J. Hazard. Mater., 182 (2010) 681–688.
[15] C.S. Liu, L.J. Zhang, F.B. Li, Y. Wang, Y. Gao, X.Z. Li, W.D. Cao, C.H. Feng, J. Dong, L.N. Sun, Dependence of sulfadiazine oxidative degradation on physicochemical properties of manganese dioxides, Ind. Eng. Chem. Res., 48 (2009) 10408–10413.
[16] J. Jiang, S.Y. Pang, J. Ma, Oxidation of triclosan by permanganate (Mn (VII)): Importance of ligands and in situ formed manganese oxide, Environ. Sci. Technol., 43 (2009) 8626–8331.
[17] C.M. Kao, K.D. Huang, J.Y. Wang, T.Y. Chen, H.Y. Chien, Application of potassium permanganate as an oxidant for in situ oxidation of trichloroethylene-contaminated groundwater: A laboratory and kinetics study, J. Hazard. Mater., 153 (2008) 919–927.
[18] E.S. Lee, P.R. Olson, N. Gupta, U. Solpuker, F.W. Schwartz, Y. Kim, Permanganate gel (PG) for groundwater remediation: Compatibility, gelation, and release characteristics, Chemosphere, 97 (2014) 140–145.
[19] J. Zhang, B. Sun, X. Guan, Oxidative removal of bisphenol A by permanganate: Kinetics, pathways and influences of co-existing chemicals, Sep. Purif. Technol., 107 (2013) 48–53.
[20] V. Gupta, S. Kumari, C. Virvadiya, Adsorption analysis of Mn(VII) from aqueous medium by activated orange peels powder, Int. Res. J. Pure Appl. Chem., 9 (2015) 1–8.
[21] K. Zhang , C. Li , J. He , R. Liu, Adsorption of permanganate onto activated carbon particles, Hua Xi Yi Ke Da Xue Xue Bao 28 (1997) 344–346.
[22] M.E. Mahmoud, A.A. Yakout, S.R. Saad, M.M. Osman, Removal of potassium permanganate from water by modified carbonaceous materials, Desal. Water Treat., 57 (2016) 15559–15569.
[23] C. Virvadiya, S. Kumari, V. Choudhary, V. Gupta, Combined bio- and chemosorption of Mn(VII) from aqueous solution by *PROSOPIS CINERARIA* leaf powder, Eur. Chem. Bull., 3 (2014) 315–318.
[24] M. Chaudhary, Use of millet husk as a biosorbent for the removal of chromium and manganese ions from the aqueous solutions, Int. J. Chem., Environ. Pharm. Res., 2 (2011) 30–33.
[25] M. Carmona, A. Pérez, A. de Lucas, L. Rodriguez, J.F. Rodriguez, Removal of chloride ions from an industrial polyethylenimine flocculant shifting it into an adhesive promoter using the anion exchange resin Amberlite IRA-420, React. Function Polym., 68 (2008) 1218–1224.
[26] S. Langergren, B.K. Svenska, Veternskapsakad Handlingar, 24 (1898) 1–39.
[27] Y.S. Ho, G. McKay, The kinetics of sorption of basic dyes from aqueous solutions by sphagnum moss peat, Can. J. Chem. Eng., 76 (1998) 822–826.
[28] M. Ozacar, I.A. Sengil, A kinetic study of metal complex dye sorption onto pinedust, Proc. Biochem., 40 (2005) 565–572.
[29] G. McKay, M.S. Otterburn, J.A. Aja, Fuller's earth and fired clay as adsorbents for dye stuffs, Water Air Soil Pollut., 24 (1985) 307–322.
[30] W.J. Weber, J.C. Morris, J. Sanity, Kinetics of adsorption on carbon from solution, Eng. Div. Am. Soc. Civil. Eng., 89 (1963) 31–59.
[31] M. Sarkar, P.K. Acharya, B. Bhaskar, Modeling the adsorption kinetics of some priority organic pollutants in water from diffusion and activation energy parameters, J. Colloid Interf. Sci., 266 (2003) 28–32.
[32] R.L. Tseng, Mesopore control of high surface area NaOH-activated carbon, J. Colloid Interf. Sci., 303 (2006) 494–502.
[33] Y.S. Ho, Effect of pH on lead removal from water using tree fern as the sorbent, Biores. Technol., 96 (2005) 1292–1996.
[34] N. Unlu, M. Ersoz, Removal characteristics of heavy metal ions onto a low cost biopolymeric sorbents from aqueous solution, J. Hazard. Mater., 136 (2006) 272–280.
[35] A. Mohammad, A.K.R. Rifaqat, A. Rais, A. Jameel, Adsorption studies on Citrus reticulata (fruit peel of orange): removal and recovery of Ni (II) from electroplating wastewater, J. Hazard. Mater., 79 (2000) 117–131.
[36] G.E. Boyd, A.W. Adamson, I. S. Myers, The exchange adsorption of ions from aqueous solutions by organic zeolites; kinetics, J. Am. Chem. Soc., 69 (1947) 2836–2848.
[37] A. Seker, T. Shahwan, A.E. Eroglu, Y. Sinan, Z. Demirel, M.C. Dalay, Equilibrium, thermodynamic and kinetic studies for the biosorption of aqueous lead (II), cadmium (II) and nickel (II) ions on Spirulina platensis, J. Hazard. Mater., 154 (2008) 973–980.
[38] B.H. Hameeda, L.H. China, S. Rengarajb, Adsorption of 4-chlorophenol onto activated carbon prepared from rattan sawdust, Desalination, 225 (2008) 185–198.
[39] M.I. Temkin, V. Pyzhev, Kinetics of ammonia synthesis on promoted iron catalysts, Acta. Physicochim., 12 (1940) 327–356.
[40] IUPAC, Compendium of Chemical Terminology, 2nd ed. (the "Gold Book") (1997). Online corrected version: (2006–) "quaternary ammonium compounds".
[41] M.M. Dubinin, E.D. Zaverina, L.V. Radushkevich, Sorption and structure of activated carbons. I investigation of organic vapor adsorption, Zh Fiz Khim., 21 (1947) 1351–1362.
[42] Y.S. Ho, J.F. Porter, G. McKay, Equilibrium isotherm studies for the sorption of divalent metal ions onto peat: copper, nickel and lead single component systems, Water Air Soil Pollut., 141 (2002) 1–33.
[43] J.M. Smith, Chemical Engineering Kinetics; McGraw-Hill: New York, 1981.